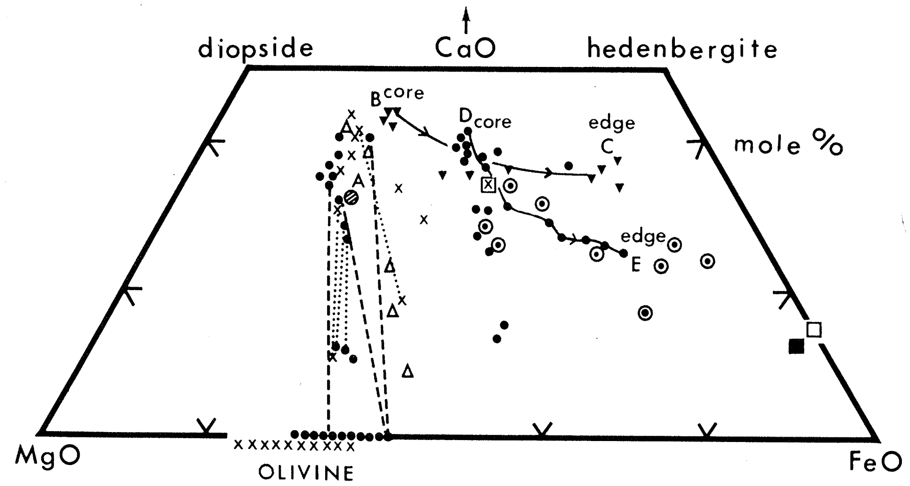

Fig. 2. Pyroxene, olivine, and pyroxenoid compositions in rocks and fines in terms of molecular percentages of CaO, MgO, and FeO. All compositions, except point *A*, are electron microprobe determinations (C. Klein and J. C. Drake, analysts). Point *A* represents the bulk analyses of the two clinopyroxenes in Table 2 (analyses 1 and 2). The symbols represent pyroxenes, olivines, and pyroxenoid in different assemblages: (solid circle) olivine and pyroxene in rock 10050,37 (fine-grained gabbro); (solid circle in ring) fine-grained, interstitial, yellowish tan pyroxene in 10050,37; (inverted solid triangle) pyroxenes in rock 10062,34 (gabbro); (open triangle) pyroxenes in rock 10045,32 (vesicular ilmenite basalt); (cross) pyroxene and olivine in fines; (cross in square) titanaugite in fines (TiO_2, 7.0 percent by weight); (solid square) yellow phase in rock 10047 similar to synthetic Ca-Fe pyroxenoid (C. W. Burnham and D. H. Lindsley, personal communication; their synthetic composition is shown by the open square). Dotted lines connect coexisting augite and pigeonite in fines and rocks. Dashed lines connect coexisting augite and olivine. Lines *B–C* and *D–E* represent probe traverses across single pyroxene grains, from core to edge (traverse length, approximately 250 μm).

6.0 percent by weight. The average plagioclase is 90 percent anorthite; the total range is from 84 to 94 percent anorthite. The anorthite probably contains some Fe in its structure. The accessory ilmenite is the main host mineral for Zr (Table 2, analysis 5). The olivines, from 58 to 70 percent forsterite, occur as rounded or bleb-like grains in clinopyroxene. Low cristobalite occurs sparingly as flattened octahedrons that are oriented microgranular inversion pseudomorphs after high cristobalite. Low tridymite occurs as inversion pseudomorphs after crystals of high tridymite, which are tabular on (0001). Both minerals show inversion twinning. Troilite, an accessory mineral, shows exsolution blebs of iron. An unidentified yellow-brown mineral containing Fe and probably Cl that decomposes under the electron beam was noted.

In microgabbro 10047 a new yellow mineral (with α 1.752, β 1.758, and δ 1.767, faintly pleochroic) consisted of CaO 6.0, FeO 47.2, MgO 0.9, MnO 1.0, Al_2O_3 0.2, TiO_2 0.5, SiO_2 45.0 percent by weight (total 100.8), corresponding to $Ca_{13}Mg_3Fe_{84}$. It has a composition similar to, and an x-ray powder pattern identical with, that of a synthetic pyroxenoid of composition $Ca_{15}Fe_{85}$ (*1*).

Impact craters produced by hypervelocity particles and ranging up to about 1 mm in diameter are common on spherules and fragments of the glass and iron-nickel in the fines. The craters have a complex morphology: in nickel-iron, a surface rim and two inner subcraters of different diameter; in glass, two subcraters, the inner with a rim of glass, a zone of granulated glass, and an outer shallow fracture crater. These impact craters are viewed as a transient event, produced while the material was in free flight in the explosion cloud of a meteorite impact in which the hypervelocity particles were themselves generated.

Well-rounded, abraded grains of glass, of plagioclase, of pyroxene, and of lithic fragments are common; they resemble terrestrial detrital sands. These features, and the rounding of large rock fragments on the lunar surface, are attributed to abrasion attending meteorite impacts. The surface material also was impacted by hypervelocity particles at the same time.

CLIFFORD FRONDEL
CORNELIS KLEIN, JR.
JUN ITO, JOHN C. DRAKE
Department of Geological Sciences,
Harvard University,
Cambridge, Massachusetts 02138

Reference and Note

1. C. W. Burnham and D. H. Lindsley, personal communication.
2. Supported by NASA contract NAS-9-8100. We thank C. W. Burnham and M. Campot for assistance.

4 January 1970

Mössbauer Spectrometry of Lunar Samples

Abstract. *Nuclear gamma resonance measurements for the nuclide ^{57}Fe in lunar material were made in transmission on lunar fines and in scattering on intact lunar rock chips. No appreciable amount of ferric iron was detected. Resonances were observed for ilmenite in all samples. Strong resonances attributed to ferrous iron in silicates, including pyroxenes and, in some samples, glasses and olivine, were also present. Metallic iron, alloyed with nickel, and troilite were also detected in the lunar fines. Differences in the spectra of various samples of lunar material and their significance are discussed.*

This paper reports on the application of Mössbauer spectrometry (*1-3*) to lunar material. Mössbauer spectrometry is appropriate for the study of solid materials that contain appreciable concentrations of elements that exhibit nuclear gamma resonance. These elements include iron, one of the major elements in the material returned to earth by Apollo 11 (*4*), and which was detected in each remote chemical analysis at Surveyor sites on the moon (*5*).

This technique has proved especially useful for the identification and characterization of iron-bearing minerals and mineraloids, determination of the phase distribution of the iron, and determination of the oxidation state of the iron in the sample. It involves the measurement of nuclear hyperfine spectra of iron atoms in the lunar material by determination of the energy spectrum of the resonance absorption of nuclear gamma radiation transmitted through

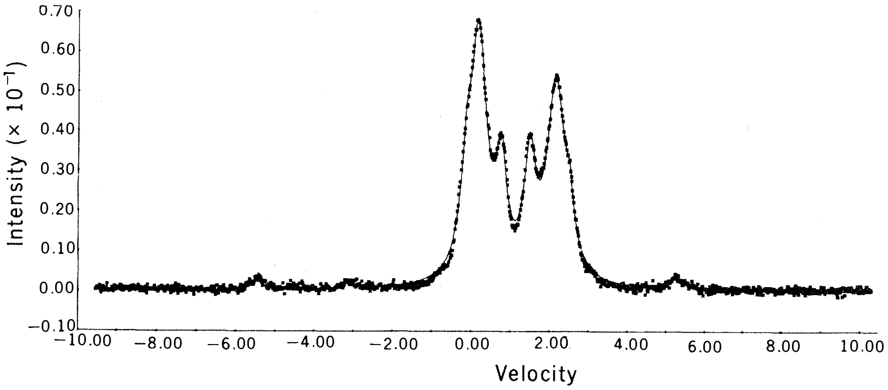

Fig. 1. Mössbauer hyperfine spectrum for unsieved documented sample lunar fines (specimen 10087,4) with least-squares computer fit (measured in transmission).

samples, or alternatively, by detection of the energy spectrum of resonantly absorbed gamma radiation from radiation reemitted from the surface of lunar specimens. These Mössbauer hyperfine spectra contain quantitative information on all major compounds containing significant amounts of iron in the sample. The method can distinguish readily among many important mineral phases, but is relatively insensitive to phases containing only trace amounts of iron.

Two general types of instruments have been used: transmission spectrometers and a scattering spectrometer. In each case, a collimated beam of gamma radiation from a radioactive source of ^{57}Co having a source strength in the 10 to 100 mc range was directed at the lunar sample. Proportional counters of several different designs were used to detect the transmitted or backscattered gamma radiation. In each case, the radioactive source was driven with a controlled periodic motion in order to provide the resonantly emitted gamma radiation with Doppler shifts of appropriate magnitude to cover the energy range of hyperfine splittings for the ^{57}Fe nuclei present in the sample. Multiscaling electronics operated in synchrony with a constant acceleration mode transducer motion provided for the recording of the number of gamma rays transmitted or scattered at each intermediate value of the Doppler shifting velocity. Mössbauer hyperfine spectra measured in this manner have permitted the analyses of terrestrial rocks for iron-bearing minerals, total iron content, and ferric to ferrous ratios. For some terrestrial samples, further useful information concerning grain size, shock exposure, radiation damage, and thermal history has been obtained (*1–3, 6*).

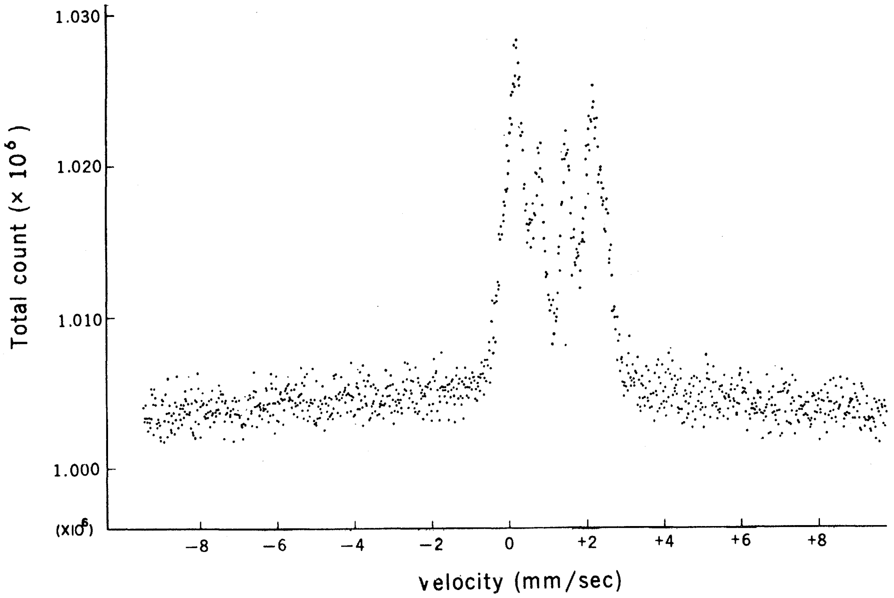

Fig. 2. Mössbauer hyperfine scattering spectrum for an interior surface of lunar rock 10020,20 (a dense fine grained crystalline rock with scattered vesicles).

The lunar fines examined included material from the documented sample and a variety of sieve size fractions from the bulk sample. Figure 1 is characteristic of the spectra obtained for lunar fines. It was measured using a specimen of approximately 70 mg of unsieved fines from the documented sample. The lunar dust covered an area of approximately 2 cm^2 corresponding to a sample thickness of about 35 mg/cm^2 between the beryllium windows. Other samples of fines ranging in sample thickness between 31 mg/cm^2 and 73 mg/cm^2 are in use. These also were completely enclosed in sample holders between thin beryllium or lucite windows. In most cases, the samples of fines in the holders have been maintained in a dry nitrogen atmosphere throughout the period of investigation.

The spectrum of Fig. 1 indicates that iron is abundant in the lunar fines and that it is distributed in a number of different phases (*1*). This sample spectrum is clearly different from the spectra of meteorites (*2*, *3*, *7*) and from the spectra of terrestrial rocks which have been examined using this technique (*1*). The most prominent peaks (near zero velocity and +2.1 mm/sec) largely originate from resonant absorption by high spin ferrous iron in the silicate phases (including iron-bearing glasses and monoclinic pyroxenes) (*1–3, 6, 8*) and by Fe^{2+} in minor opaque phases. Strong peaks are also present from ilmenite (these being located in the vicinity of +0.7 mm/sec and +1.4 mm/sec) (*1*, *9*). At higher velocities, three of the six peaks characteristic of metallic iron indicate its presence in the fines (*3*, *7*). In some samples of fines, additional low intensity peaks in the high velocity range indicate the presence of troilite (*3*, *10*).

Standard techniques of spectral analysis, including least-squares computer fitting of the spectra (*1–3*), have been used for the quantitative interpretation. Some variations both in total iron and in the distribution of iron among mineral phases have been observed between the fines of the documented sample and the fines of the bulk sample, and between different sieve size fractions of the bulk sample; however, all samples of fines which we have examined give grossly similar spectra. No major systematic trends in phase distributions were apparent in the sieve fractions from the Lunar Receiving Laboratory. In a typical sample of fines, about 73 percent of the total iron appears to be in the silicate phases, about 17 percent in ilmenite, and about 5 percent in metallic iron. Two percent or less of the total iron is typically present in troilite. We find no evidence for a significant amount of ferric iron. While our estimates of the total iron content are only approximate, we find an average of 12 percent, in good agreement with the 12.4 percent already reported (*4*) as typical for type D fines. We also find some evidence of a trend toward higher total iron content in the finer sieve fractions of the fines.

The spectral contribution from the metallic iron, which typically represents of the order of 0.5 weight percent of the fines, shows that the iron is alloyed, and the line positions and widths may be interpreted as indicating a variable composition containing some few percent nickel (*3*, *7*). This suggests a probable meteoritic origin for a significant portion of the metallic iron present in the fines. The silicate phases in the fines are rather complex, including both iron-bearing glasses of varying composition and a wide range of pyroxene compositions. These factors contribute to the exceptional width of the strongest manifest lines in the vicinity of zero velocity and +2.1 mm/sec. The presence of strong absorption attributable to iron-containing glasses is compatible with direct observations of the presence of much glassy material having high indices of refraction in the fines (*4*).

Comparison of the spectra of lunar fines exposed to air with those maintained under dry nitrogen, and with fines originally under vacuum, gave no evidence for any major changes in the lunar fines as a result of exposure to the atmosphere over a time scale of weeks, in agreement with previous observations using other techniques (*4*).

Additional measurements made on lunar fines cooled to liquid nitrogen temperature have, in general, verified the mineral phase identifications already made on the basis of measurements performed at room temperature. None of the major iron-bearing mineral phases appears to undergo a magnetic transition between 300°K and 80°K; this is in accord with the properties of the identified phases, and suggests that the contribution from certain other phases in the opaque assemblage, such as ulvöspinel (if stoichiometric), is reasonably small in these samples.

Prominent features of this material can be observed in the rock spectra (Figs. 2 and 3). Spectral differences are considerably more pronounced among the rocks than among the many samples of fines which we have examined.

Figure 2 shows a scattering spectrum measured on an interior surface of a fine grained crystalline rock (specimen 10020,20). About 25 percent of the iron in this rock appears to be in ilmenite, with the remainder mainly in the silicate phases, which include pyroxenes, some olivine and some iron-bearing glass. Our spectra show that less metallic iron is present in the type A and type B lunar rocks (including this rock) than in the fines or the breccia. Application of spectral smoothing techniques reveals evidence for some troilite.

Initial scattering measurements made on the obverse side of this rock chip (believed from circumstantial evidence to be from the bottom outer surface of the rock) show spectra grossly similar to those of the interior, which indicates a general similarity in mineralogical composition between the surface and the interior. More detailed studies of exposed surfaces are continuing, in order to examine the surface layers for radiation effects and secondary mineral formation.

The ilmenite peaks of specimen 10003,22 (Fig. 3) are relatively less intense for this rock than for the finer grained specimens, which supports the early observation (*4*) of a seemingly lower abundance of ilmenite in coarser grained rocks. There is no evidence for olivine in this rock, and iron-bearing glasses appear to be largely absent. The silicate spectrum in this rock is thus dominated by the pyroxene contributions, which exhibit relatively narrow line widths and have outer lines with unusually low relative intensities. This is indicative of appreciable ordering of the ferrous ions in the cation sites of these lunar pyroxenes, which is of special interest, as the cation distributions in pyroxenes reflect temperatures and pressures of mineral formation as well as shock exposure (*6*, *8*). While much more detailed study is required for an analysis of the thermal history of this material, our results may be interpreted as indicating a slow cooling history for this rock.

Spectra measured for the vesicular lunar basalt (rock 10022) show that about one-third of the iron in this rock is in ilmenite, which exceeds the amount in any other sample we have

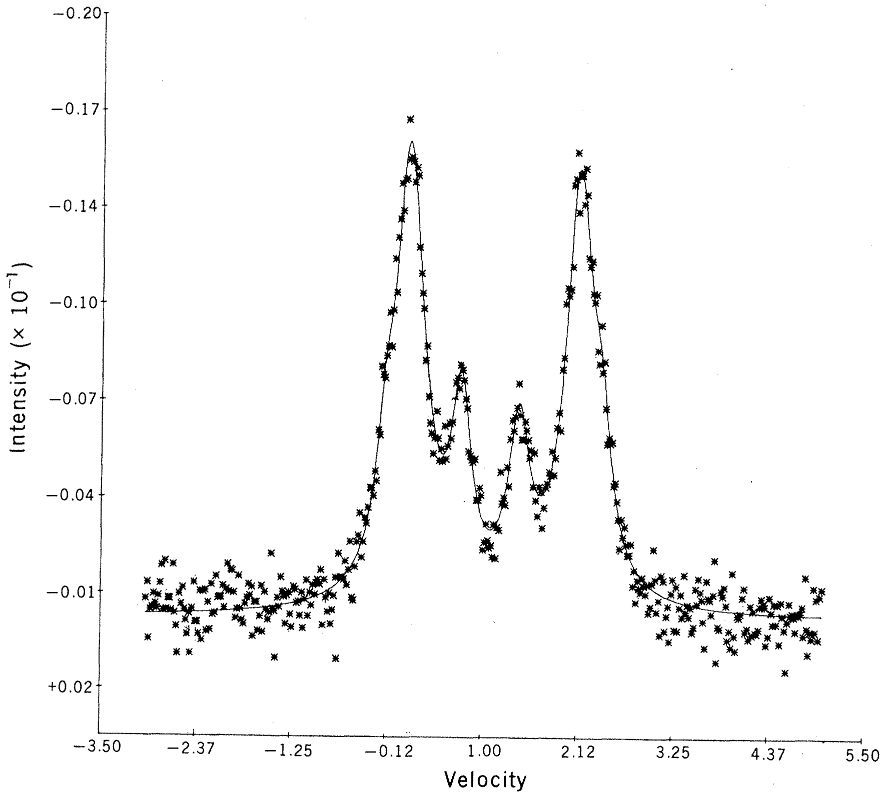

Fig. 3. Mössbauer hyperfine scattering spectrum for lunar rock 10003,22 (a gray gabbroic rock), with least-squares computer fit.

examined. The silicate phases contribute wide lines, indicating that this rock contains iron-bearing glasses in addition to pyroxenes, which is compatible with its volcanic character (*4*).

Initial scattering measurements on breccia 10065 produced spectra somewhat similar to those of the fines, as would be expected in view of the probable origin of lunar breccia as shock lithified fines (*4*); spectral differences include considerably reduced intensity in the ilmenite regions. Magnetically ordered material is present in this breccia and it seems to be primarily metallic iron (*3, 7*).

Ferric iron is largely absent from the lunar material. At most a few percent of the iron is in the Fe^{3+} state. All of the rocks and fines from Apollo 11 which we have examined appear to have an appreciable iron content and grossly similar chemical and mineralogical compositions with the individual differences as remarked upon, as evidenced by their Mössbauer spectra.

C. L. Herzenberg
D. L. Riley
IIT Research Institute, Chicago, Illinois

References and Notes

1. C. L. Herzenberg, in *Mössbauer Effect Methodology,* I. J. Gruverman, Ed. (Plenum Press, New York, in press), vol. 5; ——— and D. L. Riley, in *Developments in Applied Spectroscopy,* E. L. Grove, Ed. (Plenum Press, New York, in press), vol. 8.
2. A H. Muir, Jr., in *Mössbauer Effect Methodology,* I. J. Gruverman, Ed. (Plenum Press, New York, 1968) vol. 4, p. 75.
3. E. L. Sprenkel-Segel and G. J. Perlow, *Icarus* **8**, 66 (1968); E. L. Sprenkel-Segel and S. S. Hanna, *Geochim. Cosmochim. Acta* **28**, 1913 (1964).
4. Lunar Sample Preliminary Examination Team, *Science* **165**, 1211 (1969).

A. L. Turkevich, E. J. Franzgrote, J. H. Patterson, *ibid.* p. 2 *ibid.* **160**, 1108 (1968); *ibid.* **162**, 117 (1968); J. H. Patterson, E. J. Franzgrote, A. L. Turkevich, W. A. Anderson, T. E. Economou, H. E. Griffin, S. L. Grotch, K. P. Sowinski, *J. Geophys. Res.* **74**, 6120 (1969).

6. S. S. Hafner and D. Virgo, *Science* **165**, 285 (1969); R. W. Dundon and L. S. Walter, *Earth Planet. Sci. Lett.* **2**, 372 (1967); G. M. Bancroft and R. G. Burns, *ibid* **3**, 125 (1967).
7. L. D. Lafleur, C. D. Goodman, E. A. King, *Science* **162**, 1268 (1968).
8. G. M. Bancroft, A. G. Maddock, R. G. Burns, *Geochim. Cosmochim. Acta* **31**, 2219 (1967).
9. T. C. Gibb, N. N. Greenwood, W. Twist, *J. Inorg. Nucl. Chem.* **31**, 947 (1969); G. Shirane, D. E. Cox, W. J. Takei, S. L. Ruby, *J. Phys. Soc. Japan* **17**, 1598 (1962); Magnitudes of Doppler shift velocities are reported with respect to the center of the iron metal spectrum at room temperature, in accordance with the recommendation of the Mössbauer effect standards committee.
10. S. Hafner and M. Kalvius, *Z. Kristallogr.* **123**, 443 (1966).
11. We thank many colleagues for their contributions to this program, in particular R. B. Moler, S. I. Baker, and P. I. Flinn. We thank S. S. Hafner, A. H. Muir, and N. N. Greenwood for communicating results of their Mössbauer studies on Apollo 11 samples prior to publication. Supported by NASA contract NAS 9-8083.

4 January 1970

Mössbauer Effect and High-Voltage Electron Microscopy of Pyroxenes in Type B Samples

Abstract. *Site occupancy numbers for ferrous iron, magnesium, and calcium at the M1 and M2 sites in lunar clinopyroxenes are estimated from nuclear gamma-ray resonant absorption spectra of* ^{57}Fe*. The cation distribution is ordered; calcium and magnesium prefer M2 and M1, respectively. The distribution corresponds to an equilibrium at a temperature lower than 680°C. Crystals cleaved and sectioned by diamond-knife ultramicrotomy were examined by high-voltage (200 kv) electron microscopy and diffraction. Uniform 300- to 600-Å-wide bands that correspond to single crystal domains were found. Correlation of the bands with magnetic ordering at low temperatures is considered.*

The crystallization and subsequent cooling history of pyroxenes is reflected in their exsolution phenomenon and in the cation distribution over structural sites. Therefore, studies of the domain structure in pyroxene crystals and of the intrinsic site occupancy in the distinct phases are important (*1*).

Clinopyroxenes separated from the type B specimens 10003 and 10044 were crushed to a grain size of approximately 50 μm and further separated into fractions of different Mg,Fe,Ca compositions by means of heavy liquids. Each fraction yields a distinct resonant absorption spectrum (Fig. 1). The nuclear quadrupole doublets due to Fe^{2+} at the M1 and M2 sites are generally well resolved. The spectra of two fractions from 10044 are shown in Fig. 1. Isomer shifts and nuclear quadrupole splittings (peak to peak separation) of the clinopyroxene from rock 10044 and those of a terrestrial augite with similar chemical composition and an iron-rich orthopyroxene are given in Table 1. The widths at half peak height are approximately 0.36 mm/sec.

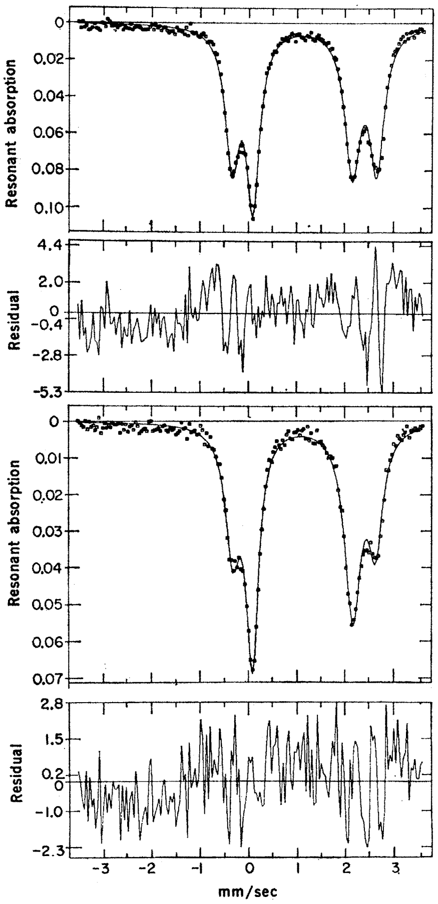

Fig. 1. Resonant absorption spectra of ^{57}Fe in clinopyroxene from specimen 10044. Upper spectrum: iron-rich fraction 10044-P3. Lower spectrum: magnesium-rich fraction 10044-P2. The solid line is a least squares fit (13 variables) to the uncorrected data. Absorbers were held at 77°K. Outer peaks: Fe^{2+} at M1; inner peaks: Fe^{2+} at M2.

The x-ray diffraction powder data indicate that the 10044 pyroxene consists almost exclusively of augite, whereas some fractions from 10003 also include pigeonite. However, measurements of isomer shifts and quadrupole splittings at 77°K in terrestrial pyroxenes with compositions within the enstatite-diopside-hedenbergite-ferrosilite quadrilateral show that the shifts and splittings are only slightly affected by small changes in Mg,Fe,Ca composition or by changes in crystal symmetry, for instance from space group $C2/c$ to $P2_1/c$. The data of Table 1 are consistent with those observations. Therefore, the resolution of the M1 and M2 doublets, for instance in the case of separates from rock 10003, is not surprising, and the hyperfine data of ^{57}Fe can be interpreted in terms of average occupancy numbers.

Average compositions and site occupancy numbers of the two chemically distinct 10044 fractions are shown in Table 2. The Mg,Fe,Ca distribution is principally an ordered one, M2 being almost exclusively occupied by Ca and Fe^{2+}, M1 being occupied by Mg and excess Fe^{2+} (Table 2). No significant Fe^{3+} peaks could be detected.

Estimates of the stability field of the observed cation distribution can be made from heating experiments. Speci-